Journal of Traditional and Complementary Medicine 11 (2021) 197–208

Contents lists available at ScienceDirect

Journal of Traditional and Complementary Medicine

journal homepage: http://www.elsevier.com/locate/jtcme

Altered presence of extra cellular matrix components in murine skin cancer: Modulation by *Azadirachta indica* leaf extract

N.A. Chugh, A. Koul*

Department of Biophysics, Basic Medical Sciences Block, Panjab University, South Campus, Sector 25, Chandigarh, 160014, India

ARTICLE INFO

Article history:
Received 2 September 2019
Received in revised form
13 February 2020
Accepted 20 March 2020
Available online 29 March 2020

Keywords:
Extra cellular matrix
Collagen
Proteoglycans
Glycosaminoglycans
Chemical carcinogenesis
Squamous cell carcinoma

ABSTRACT

Background and aim: Although, the anticancer potential of Aqueous *Azadirachta indica* leaf extract (AAILE) has been robustly established against cutaneous squamous cell carcinoma (SCC) in mice, however, its ability in modulating tumor associated extra cellular matrix (ECM) is largely unknown. Therefore, the present study was conceived to explore changes in ECM during murine skin cancer and its chemoprevention by AAILE.

Experimental procedure: Skin tumors were induced using a two-stage model of carcinogenesis employing topical application of 7,12-Dimethylbenz(a)anthracene (DMBA) and 12-O-tetradecanoyl phorbol-13-acetate (TPA) as carcinogen and promoter respectively. AAILE was administered orally to the animals. Male Laca mice were divided into four groups: control, AAILE, DMBA/TPA and AAILE + DMBA/TPA.

Results: The tumors obtained in DMBA/TPA and AAILE + DMBA/TPA groups were histologically identified as SCC. Tumor induction in these groups was accompanied by raised serum carcinoembryonic antigen (CEA) levels when compared to control counterparts. Assessment of hydroxyproline levels and histochemical staining with sirius red and trichrome stain revealed an increase in collagen in tumors of DMBA/TPA group. An increase in glycosaminoglycans (GAGs) levels was also observed in DMBA/TPA group as made evident by biochemical studies and histochemical staining using mucicarmine and alcian blue-periodic acid schiff's stain. Administration of AAILE to DMBA/TPA treated animals caused a decrease in collagen and GAG levels along with a decrease in serum CEA levels.

Conclusion: Skin tumors exhibited altered presence of ECM components which is indicative of a modified ECM. AAILE administration antagonised tumor associated ECM alterations which may be contributing to its chemopreventive activity as reported previously.

1. Introduction

The extra cellular matrix (ECM) is ubiquitously present within all tissues and organs and serves the crucial function of providing physical scaffolding for the cells. It is responsible for attributing tensile and compressive strength and elasticity to each organ. Cell adhesion to the ECM is mediated by ECM receptors which is responsible for morphological organization and other cellular functions like signal transduction and regulation of gene expression. ECM is also involved in tissue morphogenesis, differentiation and homeostasis.[1,2] Apart from the cellular changes like dysregulated proliferation, evasion of apoptosis etc, the loss of ECM control is a striking feature in tumorigenesis. The process of tumor cell invasion into the surrounding stromal tissue and at sites far from the primary site, involve interactions between the tumor cells and ECM. The dysregulated and abnormal ECM during cancer produces biochemical and biomechanical changes which forms an environment conducive for cancer progression.[3,4] The changes in ECM homeostasis occur due the imbalance between synthesis and degradation of ECM components along with their altered organisation.[5] Aberrant remodelling of ECM promotes cellular proliferation, tumor associated angiogenesis and inflammation, deregulates behaviour of stromal cells etc, thereby creating a tumorigenic environment.[3,6,7] Studies have suggested that antagonising cancer

Abbreviations: DMBA, Dimethylbenz(a)anthracene; TPA, 12-O-tetradecanoyl phorbol-13-acetate; SCC, squamous cell carcinoma; AAILE, Aqueous *Azadirachta indica* leaf extract; GAG, glycosaminoglycans; CEA, carcinoembryonic antigen.

* Corresponding author.
E-mail address: ashwanik@pu.ac.in (A. Koul).

Peer review under responsibility of The Center for Food and Biomolecules, National Taiwan University.

https://doi.org/10.1016/j.jtcme.2020.03.006

associated ECM modifications could play an important role in anticancer strategies.[8]

Non-melanoma skin cancer (NMSC) is the most common type of cancer worldwide and its incidence is persistently growing.[9,10] Squamous Cell Carcinoma (SCC) and Basal Cell Carcinoma (BCC) are the most common forms of NMSC. SCC is a cancer of the epidermal keratinocytes and starts in the upper squamous cells of the skin epidermis whereas, BCC is a cancer of the basal cells of the skin epidermis. The morbidity and mortality due to NMSC is attributable maximum to SCC because it has a greater potential to recur and metastasize to regional lymph nodes.[11] ECM alterations including increased synthesis and breakdown of matrix components (fibrous proteins and proteoglycans) has been reported during SCC in humans.[12,13] The expression and activity of matrix metalloproteinases (MMPs) and their inhibitors have been studied as prognostic indicators during skin cancer.[12] The altered expression of ECM receptors during SCC induction in mice has been linked to the appearance of early markers of tumor progression.[14] Carcinoembryonic antigen (CEA) is a highly glycosylated macromolecule which is commonly used for cancer screening and diagnosis in clinical practice. SCC patients exhibited high serum levels and immunopositivity in tumors for CEA.[15,16] Being a tumor marker, assessment of CEA levels is also done to monitor the results of treatment in clinical settings or during studies evaluating putative chemopreventive agents.[17,18]

Azadirachta indica A. Juss (*Melia Azadirachta*) commonly known as 'Neem' is well known in India and the neighbouring countries for more than 2000 years. Neem has immense medicinal value and is extensively used in ayurveda, unani and homeopathic medicine. The chemopreventive potential of *Azadirachta indica* leaf extract has been studied in several animal models of carcinogenesis including skin, forestomach, liver etc. Reports from our laboratory and those of several others have demonstrated that its anti-oncogenic activity is evident from its modulatory effects on carcinogen metabolism, oxidant-anti-oxidant defense system, cell proliferation, DNA damage, cell death, angiogenesis etc.[19–27] However, little is known about the potential of *Azadirachta indica* to modulate ECM changes accompanying cancer development. There are reports that have demonstrated that compounds isolated from this plant modulated the expression of matrix modifying enzymes including MMPs in cancer cell lines[28,29,30]; *Azadirachta indica* contains multiple active compounds that work simultaneously via different mechanisms lending support to the observed anti-cancer effects in various models of cancer.

Even though the anticancer potential of Aqueous *Azadirachta indica* leaf extract (AAILE) has been robustly established against SCC of skin, its ability in modulating the ECM changes in SCC is unknown. Invasion and metastatic dissemination of cancer cells require ECM remodelling of the primary sites and future sites of metastasis (pre-metastatic sites).[5] Thus, unraveling the ability of *Azadirachta indica* in antagonizing matrix alterations could strengthen its use as an anti-metastatic agent. Considering this, the present study was designed to study changes occurring in ECM during skin carcinogenesis and its chemoprevention by AAILE.

2. Methodology

2.1. Chemicals

7, 12 di-methylbenz(a)anthracene (DMBA); phorbol 12-myristate 13-acetate (TPA), biebrich scarlet (Ponceau BS), sirius red, chloramine-T hydrate, p-dimethylaminobenzaldehyde, dimethylmethylene blue (DMMB) were obtained from Sigma Chemical Co. (St Louis, MO, USA). Aniline blue, acid fuschin, phosphotungstic acid, phosphomolybdic acid were procured from Central Drug House (India). Hydroxy-L-proline was obtained from Himedia (India). Other chemicals used for reagent preparation were obtained from reputed Indian manufacturers (Sisco Research Laboratory, Central Drug House, SD Fine Chemicals, India) and were of highest purity/analytical grade. ELISA kit for the estimation of serum carcinoembryonic antigen level was obtained from Qayee-Bio (Shanghai, China).

2.2. Preparation of aqueous Azadirachta indica leaf extract (AAILE)

Aqueous extract of *Azadirachta indica* leaves was prepared in our laboratory according to the method described previously.[24] Fresh *Azadirachta indica* leaves were obtained from botanical garden of Panjab University, Chandigarh (India). The leaves were rinsed with water, dried and macerated in a grinder with water. This mixture was subjected to centrifugation at 2500×*g* for 10 min. The supernatant (containing water soluble components) was lyophilized to obtain a fine powder which was stored in a dark container at 4 °C for further use. The powder extract so obtained (AAILE) was reconstituted in distilled water immediately before its oral administration to the animals. Tannins, flavonoids, carbohydrates, polysaccharides and proteins were observed to be present in this extract as revealed by the phytochemical screening assays.[26] 2-'azino-bis-3-ethylbenzothiazoline-6-sulphonic acid (ABTS) and 1,1-Dipphenyl-2-picrylhydrazyl (DPPH) radical scavenging assays demonstrated concentration dependent free radical scavenging activity of this extract.[31]

2.3. Two stage model for skin tumor induction in mice

The experimental protocols involving animals were approved by the Institutional Ethics Committee and conducted according to Indian National Science Academy Guidelines. For this study, male LACA mice were procured from Central Animal House, Panjab University, Chandigarh. The animals were housed in polypropylene cages bedded with rice husk and had free access to clean drinking water and pellet diet (Ashirwad Industries Ltd, Rupnagar, Punjab). Mice were kept in well aerated conditions and a constant room temperature was maintained throughout the treatment period.

The animals were segregated into four groups (n = 10, each group) on the basis of treatment they received. Mice of group I served as control [C] and did not receive any specific treatment other than application of acetone (100 μl) [vehicle treatment]. Group II [A] animals were administered with AAILE (300 mg/kg b.w.; p.o.) for twenty-two weeks on alternate days. Group III [D] animals received a topical application of DMBA (500nmol/100 μl of acetone) for two weeks (twice weekly) followed by TPA (1.7nmol/100 μl of acetone) twice weekly for eighteen weeks on the shaved dorsal skin. Group IV [AD] animals received DMBA/TPA treatment as described for group III and were administered with AAILE as described for group II. DMBA treatment was started after two weeks of AAILE treatment. The dose for AAILE was selected based on our previous published reports[23-27]

2.4. Histopathological analysis of skin/tumors using hematoxylin and eosin staining

Hematoxylin and eosin staining was performed on paraffin embedded tissue sections[32] to ascertain the type of skin tumor formed. After completion of the treatment period (i.e. after 22 weeks of treatment) skin/skin tumors were excised and immediately transferred to neutral formalin. After 3–4 h of fixation, a cut was given to allow easier penetration of the fixative and the fixation process was continued for 12 h. Next, the tissue was dehydrated gradually in ascending series of ethanol for 1 h each. For

embedding, the dehydrated samples were placed in benzene (30 min), then sequentially in 1:1 benzene: paraffin wax, melting point 58–60 °C (1 h) and two changes of 3 h each in pure melted wax before finally embedding in paraffin wax. 5 μm thick sections were obtained using a manual hand driven microtome and transferred to albumin coated glass slides. The paraffin embedded tissue sections were dewaxed in xylene, rehydrated using descending series of alcohol, stained with hematoxylin, dehydrated using ascending series of alcohol and then stained with eosin. The stained slides were then cleared in xylene and mounted with distyrene plasticizer xylene (DPX). The sections were then viewed under light microscope (LEICA DM 3000).

2.5. Assessment of serum carcinoembryonic antigen (CEA) levels

Serum levels of CEA were assessed using the Qayee-Bio mouse CEA ELISA kit. The protocol was performed as per the kit manufacturer's instructions. The kit was based on a double-antibody sandwich ELISA method using horseradish peroxidase labelled detection method. The CEA levels in the samples were estimated from the standard curve that was plotted using the serial dilutions of the standard provided in the kit.

2.6. Analysis of collagen using histochemical stains: sirius red staining and Masson's trichrome staining

The paraffin embedded tissue sections were used for the specific staining procedures for collagen. Collagen staining using sirius red stain was performed on skin/tumors following the method described earlier.[33,34] Sirius red is used to determine the extent of total collagen in tissues and also differentiate between varying collagen types. Sirius red being an anionic dye binds to all forms of collagen. The basic amino groups of lysine and hydroxylysine and guanidine group of arginine in the collagen molecule reacts with the sulphonic groups of sirius red stain. When visualised using bright field microscopy collagen appears as bright pink to red bundles and the cells (nuclei) exhibit shades of brown.[35] Briefly, the tissue sections were dewaxed in xylene, hydrated using descending series of ethanol followed by a dip in distilled water. The sections were immersed in hematoxylin for half an hour, followed by a dip in running water and then immersed in ammonia solution for 10 s. The sections were then stained with picrosirius stain (sirius red stain prepared in picric acid solution) for 1 h, followed by a dip in acid water for 2 s and were then subjected to ascending series of ethanol. After that, tissues were cleared in xylene and mounted with DPX. The stained sections were then viewed using light microscope (LEICA DM 3000).

Collagen staining using Masson's trichome stain was performed on skin/tumors following the method described earlier.[32,36] Masson's trichrome stain is composed of the following dyes: Weigert's hematoxylin, aniline blue, biebrich scarlet and acid fuschin. Following this staining procedure, cell nuclei appear bluish-black (as stained by hematoxylin), collagen and keratin appear as blue (as stained by aniline blue) and red respectively. The tissue sections were dewaxed by immersing the slides in xylene and gradually rehydrated by using descending series of ethanol followed by a dip in distilled water. The slides were then dipped in iron alum for 5 min at 50 °C. Following this, the slides were washed in tap water for 5 min. To differentiate nuclei, slides were immersed in modified Weigert's hematoxylin for 15 min and after that washed in tap water for 10 min and distilled water for 1 min. This was followed by staining with biebrich scarlet-acid fuschin for 1 min and a dip in distilled water. Next, slides were treated with phosphomolybdic-phosphotungstic acid solution for 30 min and immediately stained with aniline blue solution for 10 min in order to stain fibroblast and collagen. After this, slides were rinsed in distilled water and differentiated with 1% acetic acid solution for 4 min. Following this, the slides were dehydrated quickly, cleared in xylene and then mounted in DPX. The stained sections were then viewed using light microscope (LEICA DM 3000).

2.7. Assessment of collagen levels using hydroxyproline assay

A colorimetric hydroxyproline assay was used to quantify collagen in skin tissues/tumors obtained after 22 weeks of treatment. This method is based on the oxidation of hydroxyproline with chloramine-T which when reacted with p-dimethylaminobenzaldehyde develops red colour.[37] The tissues were homogenized with water and treated with trichloro acetic acid for protein precipitation. The samples were then hydrolysed overnight with 6 N HCl at 110 °C. The hydrolysate was then diluted in citrate-acetate buffer, reacted with chloramine-T solution at room temperature for 20 min. This was followed by incubation with Ehrlich's solution for 15 min at 60 °C. The red colour developed was read spectrophotometrically at 550 nm. A standard curve using trans-4-hydroxy-L proline was included in each assay. The results were expressed as microgram of hydroxyproline/100 mg tissue equivalent. The collagen content was evaluated based on the fact that the weight fraction of hydroxyproline in collagen is about 13%.[38,39] A factor of 7.46 was used to convert hydroxyproline values into total collagen values.[40]

2.8. Determination of total sulphated glycosaminoglycans (GAGs) using dimethyl methylene blue (DMMB) complexation assay

A colorimetric assay was used to quantify sulphated GAGs in skin tissues/tumors obtained after 22 weeks of treatment. Tissues were digested overnight with 50 mg/ml proteinase K solution at 56 °C. Following the overnight incubation, proteinase K was inactivated by heating the sample tubes at 90 °C for 10 min. The digested tissue was used for sulphated GAG quantification using DMMB solution. The absorbance of the coloured complex formed by the GAG-DMMB complexation was measured at 520 nm and sulphated GAG quantities were determined by comparison with a calibration curve of chondroitin sulphate solution used as standard.[41,42]

2.9. Analysis of mucopolysaccharides using histochemical stains: Meyer's mucicarmine staining and alcian blue-periodic acid Schiff's staining

The paraffin embedded tissue sections were used for the specific staining procedures for mucopolysaccharides. Meyer's mucicarmine stain and alcian blue stain is used to demonstrate acidic polysaccharides. PAS stain is used for histochemical detection of neutral mucopolysaccharides.[43,44]

The tissue sections were dewaxed in xylene and hydrated through descending series of ethanol followed by a dip in distilled water. This was followed by immersing the tissue slides in alcian blue stain for 30 min, running water (2 min) and a rinse in distilled water. Then the sections were subjected to treatment with periodic acid for 5 min, washed in distilled water, followed by staining with Schiff's reagent for 10 min and a wash in running water. The sections were then dehydrated with ascending series of ethanol, cleared in xylene and mounted with DPX. The stained sections were then viewed using light microscope (Leica Microsystem-DM 3000, Leica Microsystem, Wetzlar, Germany).

For mucicarmine staining, the tissue sections were dewaxed in xylene and hydrated through descending series of ethanol followed by a dip in distilled water. This was followed by immersing the

tissue slides in Meyer's hematoxylin for 2 min, running water (2 min) and a rinse in distilled water. The sections were dipped in acid water for 10 s and washed in running tap water. The sections were then stained with mucicarmine for 50 min followed by a wash in distilled water. Dehydration was then proceeded with ascending series of ethanol, followed by clearing in xylene and mounting with DPX. The stained sections were then viewed using light microscope (Leica Microsystem-DM 3000, Leica Microsystem, Wetzlar, Germany).

2.10. Statistical analysis

For the assessment of different parameters, animals were randomly picked for analysis of carcinoembryonic antigen levels ($n = 3$), hydroxyproline, collagen and total GAG levels ($n = 4–6$). All the observations were taken into account for the data analysis. Data is expressed as mean ± SD and analysed by one-way ANOVA followed by Bonferroni's post hoc test using the SPSS software (version 14.0). $P \leq 0.05$ was considered as statistically significant.

3. Results

3.1. Skin tumor induction using two stage model-macroscopic appearance and histopathological evaluation

The application of DMBA/TPA to the depilated skin of mouse resulted in the formation of skin tumors (as exophytic growths) in DMBA/TPA and AAILE + DMBA/TPA groups, whereas, none of the mice from control and AAILE groups developed any tumors (Fig. 1). H&E staining revealed that skin from control and AAILE groups revealed uniformly arranged epidermal and dermal layers along with subcutaneous tissue. Microscopically visible inflammation was observed in the epidermis of skin from AAILE group. The tumors obtained in DMBA/TPA and AAILE + DMBA/TPA groups exhibited characteristic features of squamous cell carcinoma (SCC).[23,24,44–48] Hyperkeratosis (i.e. increased keratin formation), abnormally thickened and corrugated epidermis (infolds of epidermis) as a result of cellular hyperproliferation was prominent in tumors of DMBA/TPA group. Whorled squamous eddies (encapsulated by keratin) and extensive infiltration of cells into the dermis was also seen in these tumors. Hyperproliferative epidermis with abnormal thickening and corrugation was also observed in tumors of AAILE + DMBA/TPA group. However, the extent of hyperproliferation and hyperkeratinisation in tumors of this group was visibly less when compared to the carcinogen control (Fig. 2).

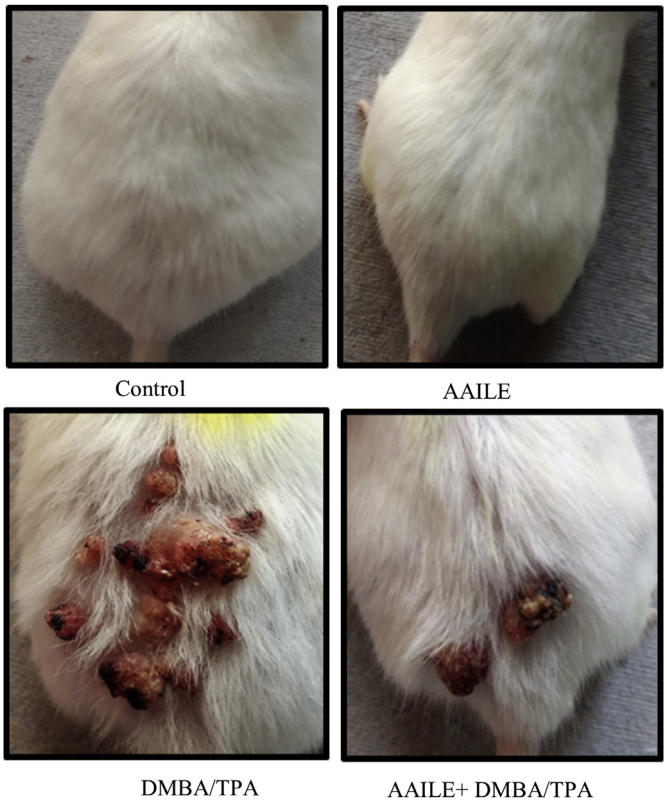

Fig. 1. Macroscopic view of skin tumors induced using two stage model of carcinogenesis. Tumors appear as exophytic growths.

3.2. Modulation of CEA levels during skin tumorigenesis and its chemoprevention by AAILE

The serum CEA levels were observed to be significantly increased in DMBA/TPA and AAILE + DMBA/TPA groups when compared to control ($p \leq 0.05$; $p \leq 0.05$) and AAILE groups ($p \leq 0.05$). AAILE administration to DMBA/TPA treated animals decreased the serum CEA levels when compared to DMBA/TPA group ($p \leq 0.05$) and increased the levels when compared to control ($p \leq 0.05$) group. No significant difference was observed in the CEA levels of control and AAILE groups (Fig. 3).

3.3. Effect of AAILE mediated chemoprevention on collagen during skin tumorigenesis

Using bright field microscopy after staining with picrosirius, collagen appeared as bright pink bundles and nuclei exhibited shades of brown to light pinkish. Skin tissues of control and AAILE groups revealed abundant presence of collagen in dermis and its absence in epidermis. The histological presence of collagen deposition in tumors from DMBA/TPA and AAILE + DMBA/TPA groups was quite different from the skin tissue sections. Consistent with the histo-architectural alterations there was no regular pattern of collagen presence (haphazard presence) as opposed to its layer specific presence in skin of control and AAILE groups. Excessive collagen deposition was observed around island of epidermal cells (transformed cells invading haphazardly) in tumors of DMBA/TPA group. However, visibly less collagen staining (low deposition) was observed in tumors of AAILE + DMBA/TPA group when compared to DMBA/TPA group (Fig. 4).

Collagen was visualised as blue bundles, cell nuclei as blackish blue and keratin as red using the trichrome stain. Skin sections from control and AAILE groups revealed regularly arranged collagen fibers in the dermis, which were absent in the epidermis indicating the prominent presence of collagen in the dermal layer. Masson's trichrome staining also revealed that there was no regular arrangement of collagen deposition in tumors from DMBA/TPA and AAILE + DMBA/TPA groups and also that collagen was present haphazardly throughout the tumor (around the tumor cells). However, the extent of collagen deposition was markedly different in the tumors from both the tumor bearing groups. The amount of collagen deposition varied in its site of histological presence as seen in the tumor sections of DMBA/TPA and AAILE + DMBA/TPA groups. Variation in the intensity of blue colour indicated that the amount of collagen deposition differed in the tumors (intra group and inter group). Although, tumors from both the groups exhibited regions of high collagen deposition, however, overall, relatively less collagen was observed in the tumors of AAILE + DMBA/TPA group when compared to tumors of DMBA/TPA group (Fig. 5).

DMBA/TPA group was observed to have a higher content of hydroxyproline when compared to control ($p \leq 0.05$) and AAILE

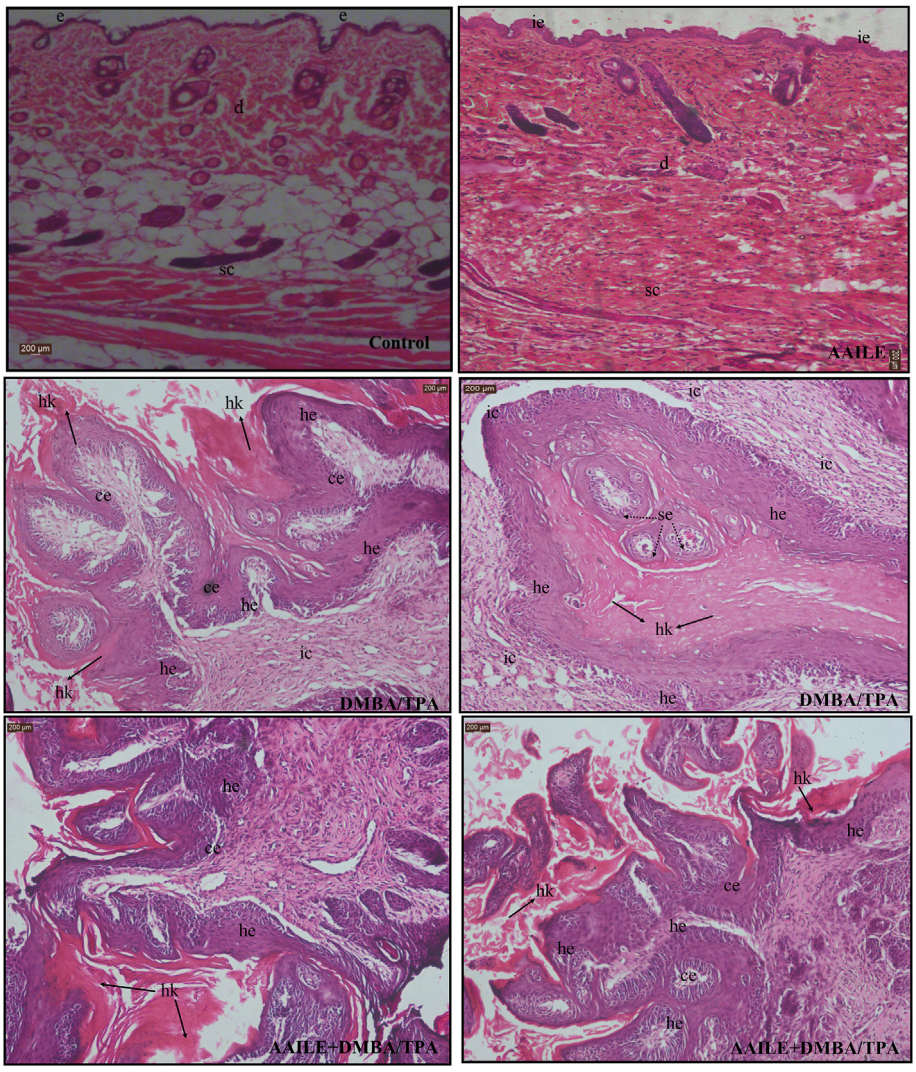

Fig. 2. Hematoxylin and Eosin stained sections of skin tumors. [e-epidermis, d-dermis, sc-subcutaneous tissue, ie-inflammation in epidermis (as evident by increase in thickness), he-hyperproliferative epidermis (hyper proliferation of epidermal cells; increase in number of hematoxylin stained nuclei), ce-corrugated epidermis (infoldings of epidermis), hk-hyperkeratosis (increased keratin formation; appear as bright pink bundles, as indicated by solid arrows), se-squamous eddies (as indicated by dashed arrows), ic-infiltrating cells].

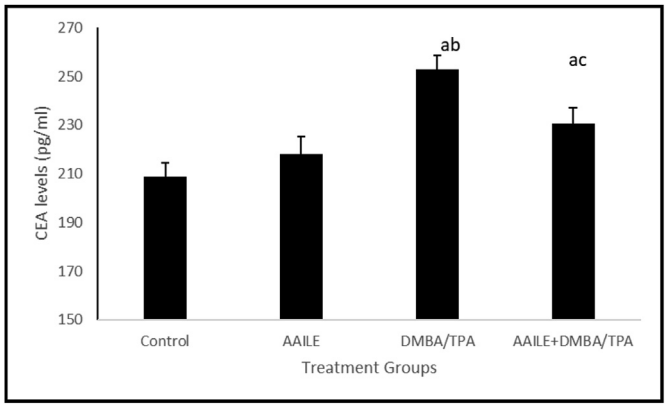

Fig. 3. Serum CEA levels during skin tumorigenesis and its chemoprevention by AAILE. Data is represented as Mean ± SD (n = 3). Data is analysed by One-Way ANOVA followed by post hoc test. [a]$p \leq 0.05$ significant with respect to control group; [b]$p \leq 0.05$ significant with respect to AAILE group; [c]$p \leq 0.05$ significant with respect to DMBA/TPA group.

($p \leq 0.05$) groups. AAILE administration to DMBA/TPA treated animals decreased the levels of hydroxyproline when compared to DMBA/TPA group ($p \leq 0.05$). No significant difference was observed in the hydroxyproline content of control, AAILE and AAILE + DMBA/TPA groups. Collagen content was evaluated considering the weight of hydroxyproline in collagen and a similar trend was observed for the collagen levels (Fig. 8a &b).

3.4. Effect of AAILE mediated chemoprevention on mucopolysaccharides/GAGs during skin tumorigenesis

Mucicarmine and alcian blue primarily stain the acidic mucopolysaccharides while periodic acid schiff's stain specifically stains the neutral polysaccharides. Sections of skin obtained from control and AAILE groups revealed mild staining for acid and neutral polysaccharides. Tumors from DMBA/TPA and AAILE + DMBA/TPA groups exhibited pronounced mucicarmine and AB-PAS staining indicating increased presence of mucopolysaccharides. AB-PAS staining revealed that tumors from DMBA/TPA group had regions with excess presence of acidic and neutral polysaccharides when

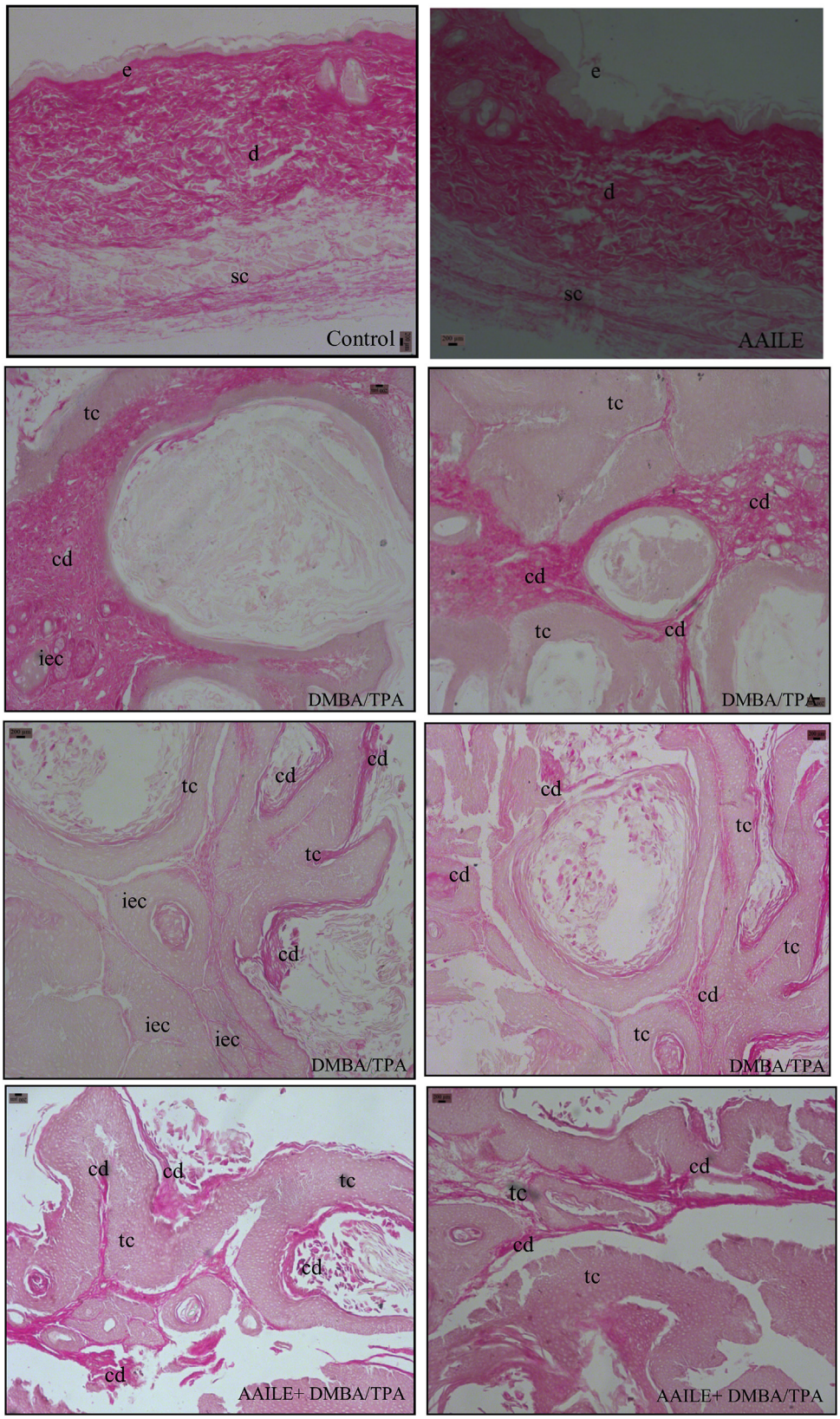

Fig. 4. Picrosirius stained sections of skin/skin tumors. (e: epidermis; d: dermis; sc: subcutaneous tissue; cd: collagen deposition; tc: tumor cells; iec: island of epidermal tumor cells; bundles of collagen fibers stained pinkish red with picrosirius stain as seen in dermis and nearly absent in epidermis of control and AAILE groups; bundles of collagen fibers stained pinkish red with picrosirius stain are seen around tumor cells in DMBA/TPA and AAILE + DMBA/TPA groups; collagen is deposited haphazardly in tumors as opposed to layer specific presence in other groups, increased collagen deposition is seen in DMBA/TPA group as compared to AAILE + DMBA/TPA group.

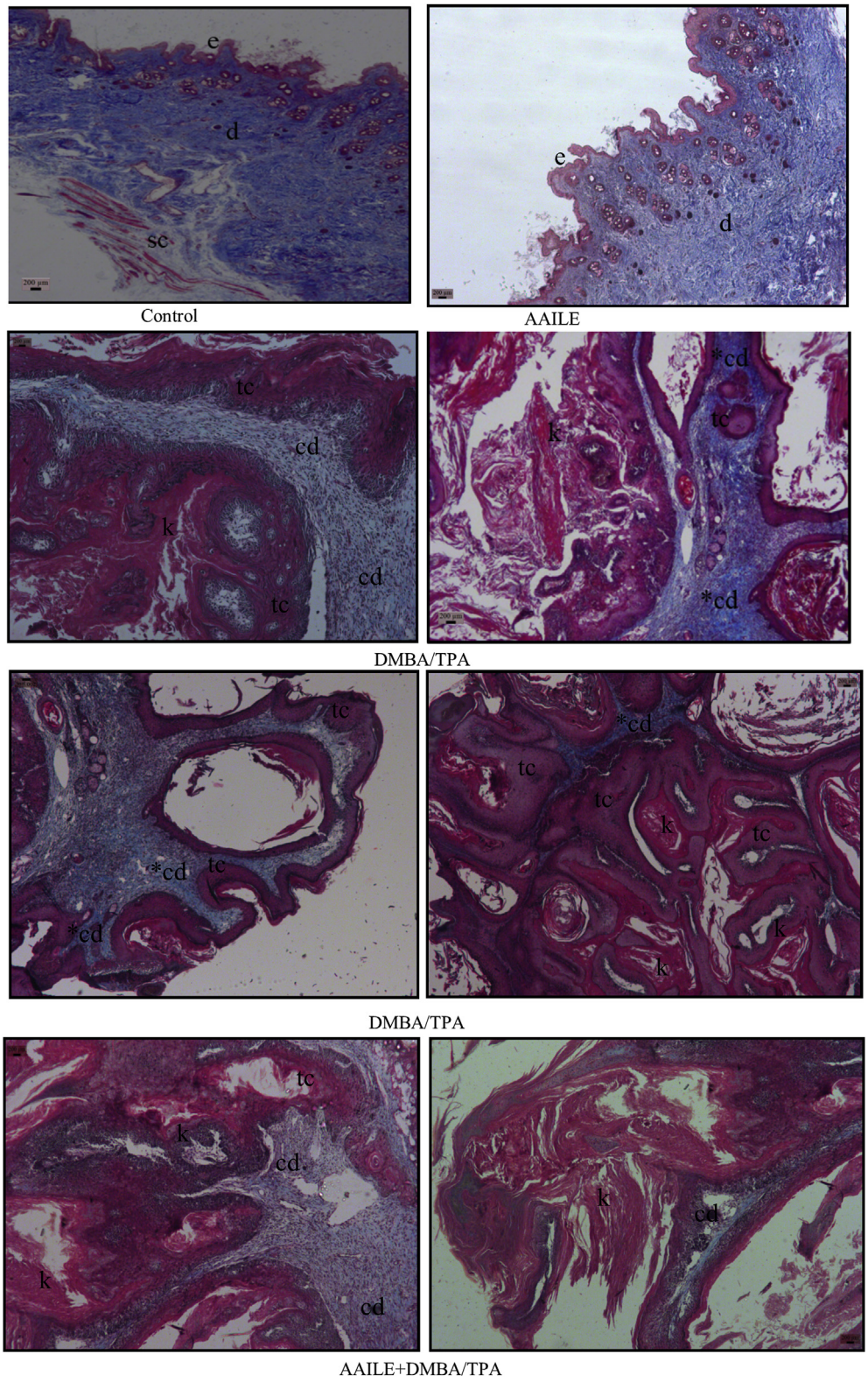

Fig. 5. Masson's Trichrome stained sections of skin/skin tumors. (e: epidermis; d: dermis; sc: subcutaneous tissue; k: keratin; nuclei stained blackish-blue; Collagen stained blue; keratin stained pinkish red; cd: collagen deposition; *cd: excessive collagen deposition; tc: tumor cells; collagen seen in dermis and keratin seen in epidermis of control and AAILE groups; haphazard presence of collagen and keratin observed in tumors of DMBA/TPA and AAILE + DMBA/TPA groups; increased collagen deposition is seen in DMBA/TPA group as compared to AAILE + DMBA/TPA group; disorderly arrangement of tumorous tissues with excessive cell proliferation is also evident).

compared to the skin sections of control and AAILE groups. However, relatively milder staining for acidic and neutral polysaccharides was observed in AAILE + DMBA/TPA group when compared to DMBA/TPA group (Figs. 6 and 7).

DMBA/TPA group was observed to have a higher content of total sulphated GAGs when compared to control ($p \leq 0.05$) and AAILE ($p \leq 0.05$) groups. AAILE administration to DMBA/TPA treated animals decreased the levels of total sulphated GAGs when compared to DMBA/TPA group ($p \leq 0.05$). No significant difference was observed in the total sulphated GAG content of control, AAILE and AAILE + DMBA/TPA groups (Fig. 8c).

4. Discussion

The ECM is not just a supportive material to the overlying cells rather it also plays a crucial role in providing spatial and temporal information to the cells by way of its constituents. The dynamic nature of ECM is exhibited by the remodelling that it undergoes during embryonic development, organ morphogenesis, wound healing, aging and several pathological conditions such as fibrosis, cancer etc.[5] The two main classes of macromolecules constituting the ECM include proteoglycans and fibrous proteins.[49,50] Increased deposition, altered organization, enhanced proteolytic activity of its constituent proteins and proteoglycans are some of the changes that occur in ECM during cancer.[5] It has been observed that many of these ECM changes have pro-carcinogenic implications.[3,4]

Amongst the fibrous proteins, collagen is the most abundant protein and serves as one of the main structural elements of the ECM, providing several functions including tensile strength, cell adhesion, chemotaxis, migration, tissue development etc.[51] Proteoglycans are characterized by the presence of large and complex carbohydrates attached to a protein core. The complex carbohydrates are referred generically as glycosaminoglycans (GAGs) or mucopolysaccharides. Proteoglycans confer buffering, hydration, binding and force-resistance properties to the ECM.

In this study, for the induction of skin tumors a two-stage model employing DMBA as a carcinogen and TPA as a promoter was used. After around eight weeks of DMBA/TPA treatment small lesions (papillomas) began to appear which increased in size and number as the treatment with the tumor promoter continued and by the

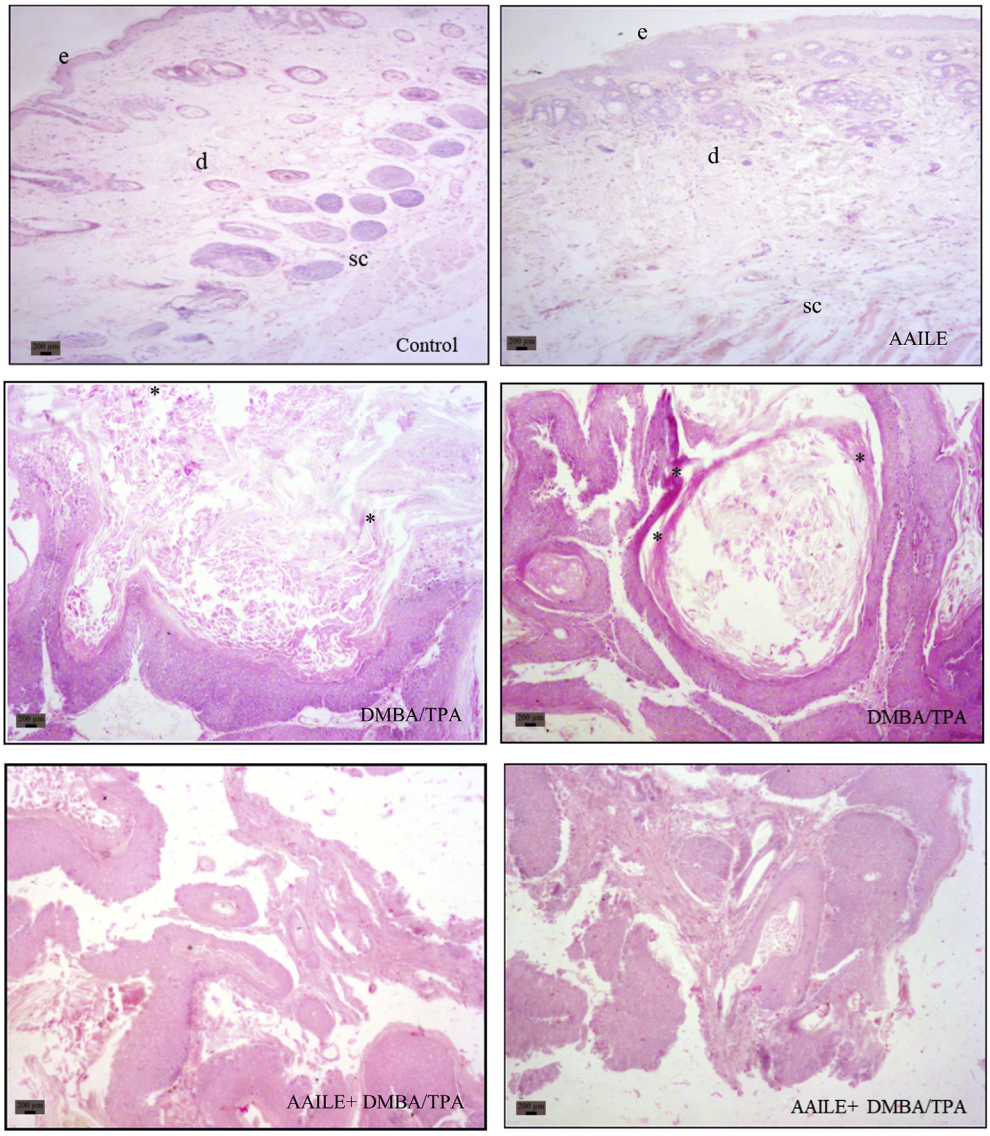

Fig. 6. Mucicarmine stained sections of skin/skin tumors. [Hematoxylin is used as a counterstain] * areas with high acidic polysaccharides. (e-epidermis, d-dermis, sc-subcutaneous tissue)

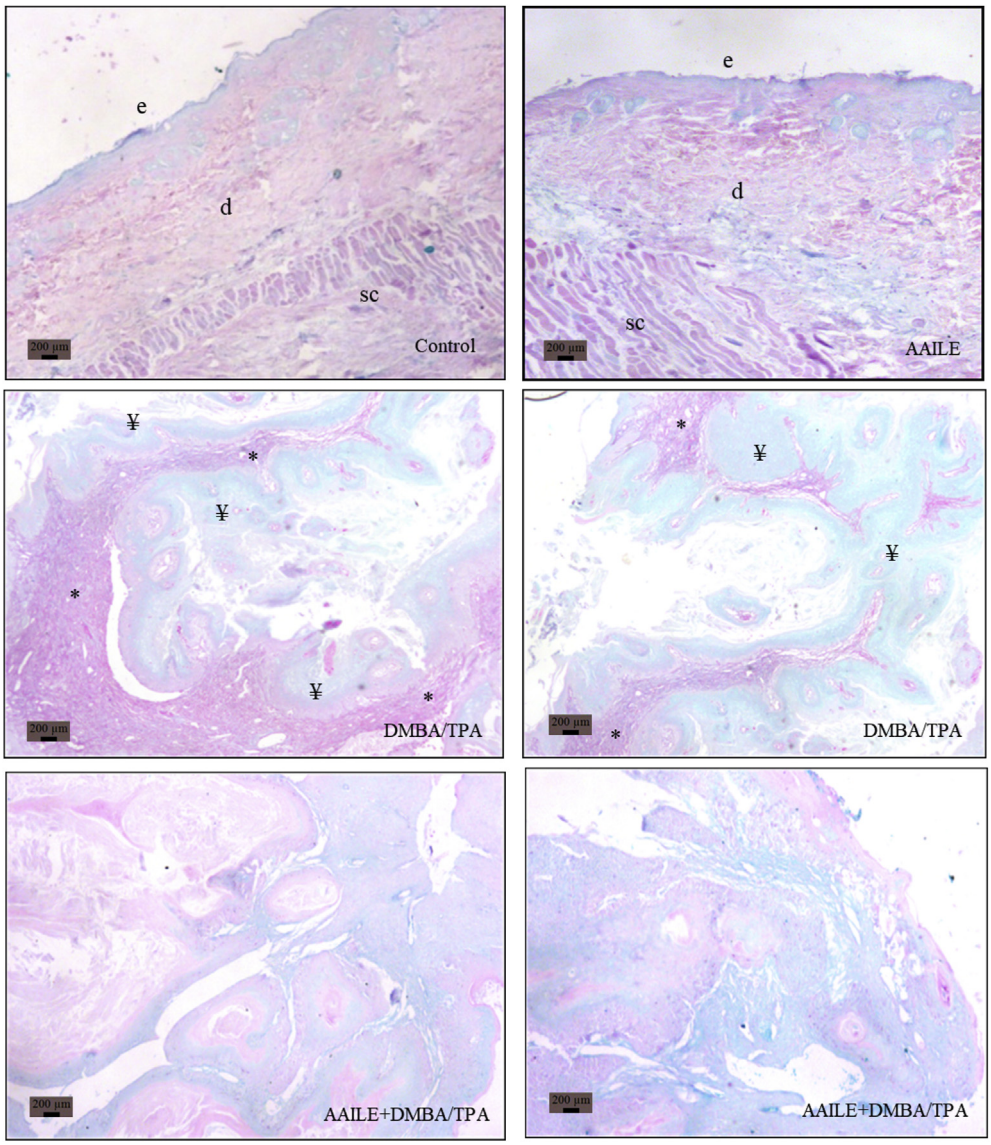

Fig. 7. AB-PAS stained sections of skin/skin tumors. (e-epidermis, d-dermis, sc-subcutaneous tissue* areas with high neutral polysaccharides [PAS stain]; ¥ areas with high acid polysaccharides [AB stain]).

end of twenty weeks of treatment with DMBA/TPA large tumors histologically identified as squamous cell carcinoma (SCC) were obtained in DMBA/TPA and AAILE + DMBA/TPA groups. We have extensively investigated the chemopreventive potential of AAILE against SCC induction using this model.[23–27,31] As previously reported by us, AAILE administration to DMBA/TPA treated animals caused reduction in tumor incidence, mean tumor volume and mean tumor burden by 41.7%, 45.6% and 54.5% respectively. The chemopreventive response of AAILE was also observed in terms of total number of tumors obtained at the end of the treatment period [32 in AAILE + DMBA/TPA group and 85 in DMBA/TPA group].[24] The characteristic features of SCC including epidermal hyperproliferation and hyperkeratinisation, presence of keratin whorls/keratin pearls, squamous eddies and infiltrating cells in the dermis were observed and are in corroboration with other reports in literature.[23,24,44–48] The microscopically visible inflammation in the epidermis of AAILE group was not associated with any deleterious effects since all the skin layers were visibly intact and seems to be a non-specific response. The increase in epidermal thickness in AAILE group was not associated with any increase in cell number as determined by micrometry and cell count studies.[27,31] This animal model of carcinogenesis has been widely used by other researchers as well to explore the potential of putative anticancer agents.[52,53] Skin tumor induction in DMBA/TPA and AAILE + DMBA/TPA groups was accompanied by an increase in serum levels of CEA. Raised levels of serum CEA and positive immunoreactivity for CEA in tumors has been observed in patients suffering from SCC.[15,16]

Drastically increased production of interstitial collagens, and several of their remodelling enzymes such as MMPs have been frequently detected in tumors and could be linked to their prognosis.[54] Hypoxia in tumors induce angiogenesis and proliferation of fibroblasts leading to excessive secretion of collagen. Also, tumor cells can dedifferentiate into fibroblasts and secrete more collagen.[55] Enhanced collagen deposition causes increased ECM stiffness which leads to up-regulation of integrin signalling and promotion of cell survival and proliferation.[56,57] As observed in the present study, tumors from DMBA/TPA group exhibited several areas of very intense staining for collagen interspersed with areas

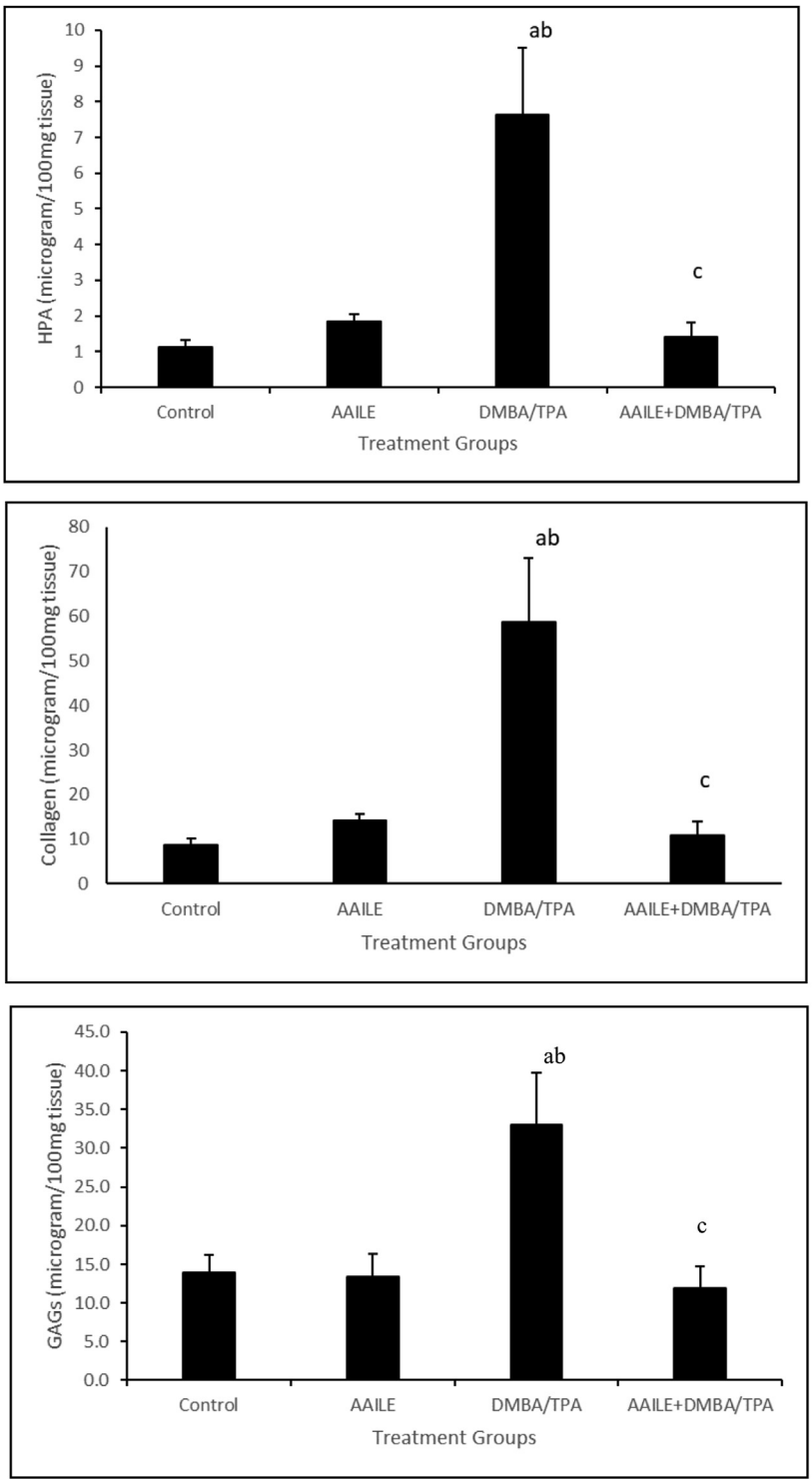

Fig. 8. Modulation in hydroxyproline, collagen and total GAG levels during skin tumorigenesis and its chemoprevention by AAILE. Data is represented as Mean ± SD (n = 4–6). Data is analysed by One-Way ANOVA followed by post hoc test. [a]p ≤0.05 significant with respect to control group; [b]p ≤ 0.05 significant with respect to AAILE group; [c]p ≤ 0.05 significant with respect to DMBA/TPA group.

of relatively less collagen deposition. Assessment of the collagen levels in tumors revealed a drastic increase in its levels in DMBA/TPA group when compared to other groups. These enhanced collagen levels decreased in the animals receiving AAILE treatment along with DMBA/TPA. The enhanced collagen levels observed in the tumors are in corroboration with previously reported studies ([3,58]; Reports have demonstrated increased collagen deposition in the ECM of cutaneous SCC in humans.[13] Rho-associated signalling has been known to upregulate collagen and proteoglycans in human SCC.[13] Skin tumors induced by DMBA/croton oil exhibited an increase in collagen levels which was reduced upon topical treatment with gallic acid (a dietary anti-oxidant).[59] A recent study from

our laboratory has revealed that DMBA/TPA induced skin tumors in mice exhibited intense staining for collagen, suggesting enhanced production of collagen in skin tumors.[44] Remodelling of ECM by employing antifibrotic therapies is gaining attention for its anti-cancer effects and could be effective in both cancer prevention and therapy. Putative anti-cancer agents have been known to inhibit cancer metastasis by their ability to reduce hydroxyproline/collagen levels.[60–63]

Abnormal expression of GAGs and proteoglycans and/or their enzymes involved in their synthesis and degradation have been known to be involved in all stages of carcinogenesis.[64] GAGs and proteoglycans control cell proliferation by acting as modulators of signal transduction. They do so by acting as co-receptors for various growth factors including tyrosine kinase receptors.[65] Sulphated GAGs such as chondroitin sulphate, heparan sulphate, etc have been implicated in cancer growth, progression and metastasis because of their interaction with growth factors, growth factor receptors and cytokines. They affect signalling cascades involved in angiogenesis, invasion and metastasis of cancer.[66–68] Heparan sulphate proteoglycans act as pro-angiogenic factors in tumors by binding to several growth factors and presenting them to their related receptors.[64,69]

Studies have revealed that substantial amounts of mucopolysaccharides/GAGs are present in tumors[70,71,44,72,73]; Histopathological studies have revealed that desmoplastic areas in carcinomas stain metachromatically with cationic dyes like alcian blue suggesting the increased presence of GAGS (hence PGs) in tumors.[74] Enhanced production of GAGs was evident in tumors of DMBA/TPA group and this decreased with the administration of AAILE. The increase in levels of total sulphated GAGs in tumors of DMBA/TPA group is in corroboration with previous reports. Tumor associated ECM has been observed to have a predominant presence of highly sulphated GAGs.[64,67] Desmoplasia in tumors is associated with recurrence, metastasis and poor prognosis.[75,76]

Anti-cancer agents target not only the intracellular defects but also modulate the tumor micro environment which comprises of immune cells, fibroblasts, endothelial cells and ECM.[55,77] A study had demonstrated that neem leaf glycoprotein mediated anti-cancer activity against murine sarcoma by normalisation of tumor microenvironment.[78] The expression of MMP 2/9 was abrogated in cancer cell lines upon treatment with nimbolide, which is a triterpenoid isolated from *A.indica*[28,29]). There are reports available in literature indicating that quercetin (a widely present phytochemical, also present in *Azadirachta indica*) has an ameliorative effect on pulmonary fibrosis which was associated with a decrease in collagen content.[79–82]

The pronounced and altered histological presence of collagen and GAGs indicated modified ECM in skin tumors of DMBA/TPA group. AAILE administration during skin tumor induction decreased the levels and modulated the histological presence of these ECM constituents indicating its ameliorative effect on dysregulated ECM. The reports from the literature and current observations of the study suggest that antagonising cancer induced ECM alterations may be contributing to its chemopreventive activity as reported previously.

Taxonomy

Cancer/Oncology, Preclinical studies, Chemical carcinogenesis and its phytomodulation.

Declaration of competing interest

The authors declare that they, have no known competing financial interests or personal relationships. that could have appeared to influence the work reported in this paper.

Acknowledgment

The authors thank the Indian Council of Medical Research (ICMR), New Delhi, India, for providing the financial assistance to carry out the present work (File No: 45/44/2014/BMS/TRM).

References

1. Harburger DS, Calderwood DA. Integrin signalling at a glance. *J Cell Sci*. 2009;122:159–163.
2. Xian X, Gopal S, Couchman JR. Syndecans as receptors and organizers of the extracellular matrix. *Cell Tissue Res*. 2010;339:31–46.
3. Lu P, Weaver VM, Werb Z. The extracellular matrix: a dynamic niche in cancer progression. *J Cell Biol*. 2012;196:395–406.
4. Venning FA, Wullkopf L, Erler JT. Targeting ECM disrupts cancer progression. *Front. Oncol*. 2015;5:224.
5. Cox TR, Erler JT. Remodeling and homeostasis of the extracellular matrix: implications for fibrotic diseases and cancer. *Dis. Model. Mech*. 2011;4:165–178.
6. Campbell NE, Kellenberger L, Greenaway J, Moorehead RA, Linnerth-Petrik NM, Petrik J. Extracellular matrix proteins and tumor angiogenesis. *J. Oncol*.. 2010: 13. Article ID 586905.
7. Bonnans C, Chou J, Werb Z. Remodelling the extracellular matrix in development and disease. *Nat Rev Mol Cell Biol*. 2014;15(12):786–801.
8. Harisi R, Jeney A. Extracellular matrix as target for antitumor therapy. *Onco-Targets Ther*. 2015;8:1387–1398.
9. Lardaro T, Shea SM, Sharfman W, Liégeois N, Sober AJ. Improvements in the staging of cutaneous squamous-cell carcinoma in the 7th edition of the AJCC Cancer Staging Manual. *Ann Surg Oncol*. 2010;17, 1979-1080.
10. Le MN, Lee E, Singh B. The evolution of staging of cutaneous squamous cell carcinomas: a structured review. *IJHNS*. 2017;8:57–63.
11. Riffat F, Palme CE, Veness M. *Non-melanoma Skin Cancer of the Head and Neck. Head and Neck Cancer Clinics*. New Delhi: Springer; 2015.
12. Kerkelä E, Saarialho-Kere U. Matrix metalloproteinases in tumor progression: focus on basal and squamous cell skin cancer. *Exp Dermatol*. 2003;12:109–125.
13. Ibbetson SJ, Pyne NT, Pollard AN, Olson MF, Samuel MS. Mechano transduction pathways promoting tumor progression are activated in invasive human squamous cell carcinoma. *Am J Pathol*. 2013;183:930–937.
14. Tennenbaum T, Yuspa SH, Grover A, et al. Extracellular matrix receptors and mouse skin carcinogenesis: altered expression linked to appearance of early markers of tumor progression. *Canc Res*. 1992;52(10):2966–2976.
15. Ramezani M, Mohamadzaheri E, Khazaei S, et al. Comparison of EMA, CEA, CD10 and Bcl-2 biomarkers by immunohistochemistry in squamous cell carcinoma and basal cell carcinoma of the skin. *Asian Pac J Cancer Prev*. 2016;17: 1379–1383.
16. Latteri S, Catania VE, Malaguarnera G, et al. Carcinoembryonic antigen serum levels in nonmelanoma skin cancer. *Biomedicine*. 2018;6(1):24.
17. Latteri S, Malaguarnera G, Mannino M, et al. Ultrasound as point of care in management of polytrauma and its complication. *J. Ultrasound*. 2017;20: 171–177.
18. Mohan V, Koul A. Anticancer potential of Tinospora cordifolia and arabinogalactan against benzo(a)pyrene induced pulmonary tumorigenesis: a study in relevance to various biomarkers. *J Herbmed Pharmacol*. 2018;7(4):225–235.
19. Gangar SC, Koul A. *Azadirachta indica* leaf extract modulates initiation phase of murine forestomach tumorigenesis. *Indian J Biochem Biophys*. 2007;44: 209–215.
20. Roy MK, Kobori M, Takenaka M. Antiproliferative effect on human cancer cell lines after treatment with Nimbolide extracted from an edible part of the neem tree (*A. indica*). *Phytother Res*. 2007;21:245–250.
21. Gangar SC, Koul A. Histochemical, ultrastructural and biochemical evidences for *Azadirachta indica* induced apoptosis in benzo(a)pyrene induced murine forestomach tumors. *J Environ Pathol Toxicol Oncol*. 2008;27:219–232.
22. Kumar GH, Chandra Mohan KV, Jagannadha RA, Nagini S. Nimbolide a limonoid from Azadirachta indica inhibits proliferation and induces apoptosis of human choriocarcinoma (BeWo) cells. *Invest N Drugs*. 2009;27(3):246–252.
23. Arora N, Bansal MP, Koul A. *Azadirachta indica* exerts chemopreventive action against murine skin cancer: studies on histopathological, ultra-structural changes and modulation of NF-kappa B, AP-1 and STAT1. *Oncol Res*. 2011a;19:179–191.
24. Arora N, Koul A, Bansal MP. Chemopreventive activity of *Azadirachta indica* on two stage skin carcinogenesis in murine model. *Phytother Res*. 2011b;25: 408–416.
25. Arora N, Bansal MP, Koul A. Modulatory effects of *Azadirachta indica leaf* extract on cutaneous and hepatic biochemical status during promotion of DMBA/TPA induced skin tumorigenesis in mice. *Indian J Biochem Biophys*. 2013a;50: 105–113.
26. Arora N, Bansal MP, Koul A. *Azadirachta indica* acts as a pro-oxidant and modulates cell cycle associated proteins during DMBA/TPA induced skin carcinogenesis in mice. *Cell Biochem Funct*. 2013b;31:385–394.
27. Chugh NA, Bansal MP, Koul A. The effect of *Azadirachta indica* leaf extract on early stages of chemically induced skin cancer in mice. *JHSMP*. 2018;24: 257–271.
28. Babykutty S, Priya PS, Nair MA, Srinivas P, Gopala S. Nimbolide retards tumor

cell migration, invasion, and angiogenesis by downregulating MMP-2/9 expression via inhibiting ERK1/2 and reducing DNA-binding activity of NF-κB in colon cancer cells. *Mol Carcinog*. 2012;51:475–490.
29. Gupta SC, et al. Modification of cysteine 179 of IkBα Kinase by Nimbolide leads to down regulation of NF-kB regulated cell survival and proliferative proteins and sensitization of tumor cells to chemotherapeutic agents.**Erratum in:** J Biol Chem. 2012; 287(15):12152. *J Biol. Chem*. 2010;285(46):35406–35417.
30. Elumalai P, Brindha Mercy A, Arunkamar R, et al. Nimbolide inhibits invasion and migration, and down-regulates uPAR chemokine gene expression, in two breast cancer cell lines. *Cell Prolif*. 2014;47(6):540–552.
31. Koul A, Bharati S, Arora N. *Azadirachta indica* exerts phytopreventive action in initial stages of skin and hepatic tumorigenesis. *Panjab Univ. Res. J. (Sci)*. 2013;63:77–89.
32. Humanson LG. *Animal Tissue Technique*. second ed. San Francisco, U.S.A: W. H. Freeman and Company; 1961.
33. Puchtler H, Waldrop FS, Valentine LS. Polarisation microscopic studies of connective tissue stained with picrosirius red FBA. *Beitrdge Zur Pathologie*. 1973;150:174–187.
34. Junqueira LCU, Bignolas G, Brentani RR. Picrosirius staining plus polarization microscopy: a specific method for collagen detection in tissue sections. *Histochem J*. 1979;11:447–455.
35. Bhutda S, Surve MV, Anil A, et al. Histochemical staining of collagen and identification of its subtypes by picrosirius red dye in mouse reproductive tissues. *Bio-protocol*. 2017;7(21), e2592.
36. Carson Freida L. *Histology, A Self-Instructional Text*. 1990:142–144.
37. Edwards CA, Brien Wd O. Modified assay for determination of hydroxyproline in a tissue hydrolysate. *Clin Chim Acta*. 1980;104:161–167.
38. Gullino PM, Grantham FH, Clark SH. The collagen content of transplanted tumors. *Canc Res*. 1962;22:1031–1037.
39. Ignat'eva NY, Danilov NA, Averkiev SV, Obrezkova MV, Lunin VV, Sobol EN. Determination of hydroxyproline in tissues and the evaluation of the collagen content of the tissues. *J Anal Chem*. 2007;62:51–57.
40. Neuman RE, Logan MA. The determination of collagen and elastin in tissues. *J Biol Chem*. 1950;186(2):549–556.
41. Barbosa I, Garcia S, Barbier-Chassefiere V, Caruelle JP, Martelly I, Papy-Garcia. Improved and simple micro assay for sulphated glycosaminoglycans quantification in biological extracts and its use in skin and muscle tissue studies. *Glycobiology*. 2003;13(9):647–653.
42. Coulson-Thomas VJ, Gesteira TF. *Dimethylmethylene Blue Assay*. 4. 2014:1–4, 18 http://www.bio-protocol.org/e1236.
43. Koul A, Bala S, Yasmeen Arora N. *Aloe vera* affects changes induced in pulmonary tissue of mice caused by cigarette smoke inhalation. *Environ Toxicol*. 2015;30:999–1013.
44. Koul A, Bansal MP, Aniqa, Chaudhary H, Chugh NA. Lycopene enriched tomato extract suppresses chemically induced skin tumorigenesis in mice. *IJVNR*. 2019. https://doi.org/10.1024/0300-9831/a000597.
45. Dhawan D, Balasubramaniam B, Amonkar JA. Chemopreventive effect of 4-demethyl epidophyllotoxin on DMBA/TPA induced mouse skin carcinogenesis. *Carcinogenesis*. 1999;20(6):997–1003.
46. Prakash J, Gupta SK, Dinda AK. *Withania somnifera* root extract prevents DMBA-induced squamous cell carcinoma of Skin in swiss albino mice. *Nutr Canc*. 2002;42(1):91–97.
47. Padmavathi B, Rath PC, Rao AR. Roots of *Withania somnifera* inhibit forestomach and skin carcinogenesis in mice. *Evi Based Complemen Altern Med*. 2005;2(1):99–105.
48. Sati J, Mohanty BP, Garg ML, Koul A. Pro-oxidant role of silibinin in DMBA/TPA induced skin cancer: 1H NMR metabolomic and biochemical study. *PloS One*. 2016;11, e0158955.
49. Jarvelainen H, Sainio A, Koulu M, Wight TN, Penttinen R. Extracellular matrix molecules: potential targets in pharmacotherapy. *Pharmacol Rev*. 2009;61:198–223.
50. Schaefer L, Schaefer RM. Proteoglycans: from structural compounds to signalling molecules. *Cell Tissue Res*. 2010;339:237–246.
51. Rozario T, DeSimone DW. The extracellular matrix in development and morphogenesis: a dynamic view. *Dev Biol*. 2010;341:126–140.
52. Roduan MRM, Hamid RA, Sulaiman H, Mohtarrudin N. Annona muricata leaves extracts prevent DMBA/TPA-induced skin tumorigenesis via modulating antioxidants enzymes system in ICR mice. *Biomed Pharmacother*. 2017;94:481–488.
53. Kong YH, Xu SP. Salidroside prevents skin carcinogenesis induced by DMBA/TPA in a mouse model through suppression of inflammation and promotion of apoptosis. *Oncol Rep*. 2018;39:2513–2526.
54. Noel A, Gutierrez-Fernandez A, Sounni NE, et al. New and paradoxical roles of matrix metalloproteinases in the tumor microenvironment. *Front Pharmacol*. 2012;3:140.
55. Egeblad M, Nakasone ES, Werb Z. Tumors as organs: complex tissues that interface with the entire organism. *Dev Cell*. 2010;18:884–901.
56. Paszek MJ, Zahir N, Johnson KR, et al. Tensional homeostasis and the malignant phenotype. *Canc Cell*. 2005;8:241–254.
57. Levental KR, Yu H, Kass L, et al. Matrix crosslinking forces tumor progression by enhancing integrin signaling. *Cell*. 2009;139:891–906.
58. Provenzano PP, et al. Collagen density promotes mammary tumor initiation and progression. *BMC Med*. 2008;6(11). https://doi.org/10.1186/1741-7015-6-11.
59. Subramanian V, Venkatesan B, Tumala A, Vellaichamy E. Topical application of Gallic acid suppresses the 7, 12-DMBA/Croton oil induced two-step skin carcinogenesis by modulating anti-oxidants and MMP-2/MMP-9 in swiss albino mice. *Food Chem Toxicol*. 2014;66:44–55.
60. Pradeep CR, Kuttan G. Effect of beta-carotene on the inhibition of lung metastasis in mice. *Phytomedicine*. 2003;10(2-3):159–164.
61. Prabhu VV, Guruvayoorappan C. Inhibition of metastatic lung cancer in C57BL/6 mice by marine mangrove Rhizophora apiculata. *Asian Pac J Cancer Prev APJCP*. 2013;14(3):1833–1840.
62. Shathish K, Sakthivel KM, Guruvayoorappan C. Protective effect of solanum muricatum on tumor metastasis by regulating inflammatory mediators and nuclear factor-kappa B subunits. *J Environ Pathol Toxicol Oncol*. 2015;34(3):249–262.
63. George GK, Kuttan G. Inhibition of pulmonary metastasis by Emilia sonchifolia (L.) DC: an in vivo experimental study. *Phytomedicine*. 2016;15(2):123–130, 23.
64. Theocharis AD, Skandalis SS, Tzanakakis GN, Karamanos NK. Proteoglycans in health and disease: novel roles for proteoglycans in malignancy and their pharmacological targeting. *FEBS J*. 2010;277:3904–3923.
65. Bernfield M, Gotte M, Park PW, et al. Functions of cell surface heparin sulfate proteoglycans. *Annu Rev Biochem*. 1999;68:729–777.
66. Volpi N. Therapeutic applications of glycosaminoglycans. *Curr Med Chem*. 2006;13:1799–1810.
67. Afratis N, Gialeli C, Nikitovic D, et al. Glycosaminoglycans: key players in cancer cell biology and treatment. *FEBS J*. 2012;279:1177–1197.
68. Morla S. Glycosaminoglycans and glycosaminoglycan mimetics in cancer and inflammation. *Int J Mol Sci*. 2019;20:1963. https://doi.org/10.3390/ijms20081963.
69. Iozzo RV. Heparan sulfate proteoglycans: intricate molecules with intriguing functions. *J Clin Invest*. 2001;108:165–167.
70. Warner KA, Adams A, Bernardi L, et al. Characterization of tumorigenic cell lines from the recurrence and lymph node metastasis of a human salivary mucoepidermoid carcinoma. *Oral Oncol*. 2013;49:1059–1066.
71. Koh HM, Maeng YH, Jang BG, Choi JH, Lim Hyun C. A rare case of nodular mucinosis of the breast. *J. Pathol. Transl. Med*. 2017;51:332.
72. Pinho SS, Reis CA. Glycosylation in cancer: mechanisms and clinical implications. *Nat Rev Canc*. 2015;15:540.
73. Cserni G, Floris G, Koufopoulos N, et al. Invasive lobular carcinoma with extracellular mucin production—a novel pattern of lobular carcinomas of the breast. Clinico-pathological description of eight cases. *Virchows Arch*. 2017;8:1–10.
74. Iozzo V, Sanderson RD, Renato J. Proteoglycans in cancer biology, tumour microenvironment and angiogenesis. *Cell. Mol. Med*. 2011;15(5):1013–1031.
75. Hideki U, Yukihide K, Shigeki S, et al. Desmoplastic pattern at the tumor front defines poor-prognosis subtypes of colorectal cancer. *Am J Surg Pathol*. 2017;41(11):1506–1512.
76. Breuninger H. Desmoplastic SCC of skin and vermilion surface. *Cancer*. 1997;79(5):915–919.
77. Prager GW, Poettler M, Unseld M, Zielinski CC. Angiogenesis in cancer: anti-VEGF escapes mechanisms. *Transl Lung Cancer Res*. 2012;1:14–25.
78. Barik S, Banerjee S, Mallick A, et al. Normalization of tumor microenvironment by neem leaf glycoprotein potentiates effector T cells functions and therapeutically intervenes in the growth of mouse sarcoma. *PloS One*. 2013;8(6), e66501.
79. Long X, Zeng X, Zhang FQ, Wang XJ. Influence of quercetin and x-ray on collagen synthesis of cultured human keloid-derived fibroblasts. *Chin Med Sci J*. 2006;21:179–183.
80. Baowen Q, Yulin Z, Xin W, et al. A further investigation concerning correlation between anti-fibrotic effect of liposomal quercetin and inflammatory cytokines in pulmonary fibrosis. *Eur J Pharmacol*. 2010;642:134–139.
81. Nakamura T, Matsushima M, Hayashi Y, et al. Attenuation of transforming growth factor-β-stimulated collagen production in fibroblasts by quercetin-induced heme oxygenase-1. *Am J Respir Cell Mol Biol*. 2011;44:614–620.
82. Verma R, Kushwah L, Gohel D, Patel M, Marvania T, Balakrishnan S. Evaluating the ameliorative potential of quercetin against the bleomycin-induced pulmonary fibrosis in wistar rats. *Pulm Med*. 2013;2013:1–10.